Lithuanian Journal of Physics, Vol. **46**, No. 4, pp. 425–431 (2006) doi:10.3952/lithjphys.46415

MONITORING OF $L_{2,3}$ X-RAY EMISSION OF TRANSITION ELEMENT ATOMS NEAR $2p$ THRESHOLD

A. Kynienė, S. Kučas, R. Karazija

Institute of Theoretical Physics and Astronomy of Vilnius University, A. Goštauto 12, LT-01108 Vilnius, Lithuania
E-mail: kyniene@itpa.lt

Received 30 November 2006

The variation of the $L_{2,3}$ emission spectra in dependence on photoexcitation energy is considered and interpreted for atoms of three elements Sc, Fe, and Ni correspondingly at the beginning, at the middle, and at the end of $3d$ transition group. The population of levels after the resonant photoexcitation and the subsequent radiative transitions have been calculated in configuration mixing approximation.

Keywords: $3d$ transition elements, photoexcitation, emission spectra

PACS: 32.30.Rj, 32.80.Hd, 32.80.Fb

1. Introduction

The construction of bright sources of X-rays opens the new possibilities for the investigation of X-ray absorption and emission spectra, especially of less intensive spectra of free atoms. Recently the monochromatised synchrotron radiation and the atomic beam technique were used to study the photoabsorption of vapours of the most $3d$ transition elements in the region of $2p$ resonances [1–4]. The corresponding photoexcitation and photoelectron spectra contain a complex structure, which is reliably interpreted by the theoretical calculations taking into account the s–d mixing and for some elements even by the single-configuration quasirelativistic Hartree–Fock approximation.

Traditionally the X-ray emission spectra are generated by photoexcitation of the inner electronic shell. Using the monochromatised radiation the emission spectrum can be obtained by exciting atoms into a narrow interval of discrete levels and in such a way monitoring the emission near the ionization threshold. This new type of spectra for ionic compounds of some $3d$ elements near $2p$ threshold was registered in [5, 6]. The results of calculation of $L_{2,3}$ emission spectra for free Mn reproduced the variation of intensities, positions, and fine structure of maxima. The atomic calculations for Cr and Fe also enabled us to explain some properties of the resonant emission of these metals.

The aim of this work is to investigate theoretically the variation of the emission spectra of free atoms of $3d$ elements when exciting them by X-rays, corresponding to some more intensive photoexcitation lines or their groups. Such spectra are not registered yet, but the successful application of the approximation used for the interpretation of the photoexcitation and photoelectron spectra of free atoms of these elements as well as of the emission spectra of Mn compounds allow us to expect the reliability of the calculated spectra.

2. Method of calculation

The investigation of photoabsorption and emission spectra has been performed for the three elements with different number of electrons in the $3d^N$ shell: Sc $3d4s^2$, Fe $3d^64s^2$, and Ni $3d^84s^2$. For the evaporation of $3d$ transition metals and formation of atomic beams rather high temperatures of 1000–1800 K are necessary. We have chosen the same temperatures which were used for the registration of photoabsorption spectra: 1600 K for Sc, 1750 K for Fe, and 1800 K for Ni [1, 3, 7]. At these temperatures the thermal population of all levels of the ground term and for Ni also the population of the ground term of other low-lying configuration $3d^94s^2$ must be taken into account.

The spectral width of the exciting X-ray beam in the experimental investigation of $L_{2,3}$ emission spectra of $3d$ element compounds was taken equal to 0.53 eV, but in the theoretical investigation some intervals were insignificantly enlarged in order to include all the group

ISSN 1648-8504

Table 1. Average natural width for the levels of $3d$ transition atoms with the $2p_j^{-1}$ vacancy.

Element	Configuration (apart from $2p_j^{-1}$)	Average width, eV	
		$2p_{3/2}^{-1}$	$2p_{1/2}^{-1}$
Sc	$3d^2 4s^2$	0.26	0.26
Ti	$3d^3 4s^2$	0.33	0.33
V	$3d^4 4s^2$	0.36	0.38
Cr	$3d^5 4s^2$	0.39	0.41
Mn	$3d^6 4s^2$	0.43	0.47
Fe	$3d^7 4s^2$	0.46	0.56
Co	$3d^8 4s^2$	0.51	0.73
Ni	$3d^9 4s^2$	0.56	1.09
Cu	$3d^{10} 4s^2$	0.62	1.37

of neigbouring lines [5]. Here we follow the same prescription.

All calculations have been performed in quasirelativistic approximation using the Cowan code [8]. As usually for such elements the Coulomb integrals have been scaled down to 80% of their *ab initio* values.

The strong spin–orbit interaction of the $2p^{-1}$ vacancy splits the energy spectrum of excited $2p^5 3d^{N+1}$ configurations into L_2 and L_3 groups separated approximately by 5–17 eV. Due to the Coulomb interaction between the $2p^{-1}$ vacancy and $3d^N$ shell, as well as within this shell, the L_2 and L_3 spin–orbit groups of levels overlap in Sc, they are separated by a small gap in Fe, and well separated only for Ni.

The energy spectra of configurations, corresponding to $3d$–$4s$ excitations, overlap between them, thus the s–d mixing must be taken into account. For Sc and Ni some additional configurations have been included, too.

The $2p$ resonances in photoabsorption spectrum are mainly determined by $2p$–$3d$ excitation into the open $3d^N$ shell [1–4].

The excited levels of atoms with open electronic shells have different natural width. However, it was demonstrated in [5, 9] that in the calculations of X-ray excitation and emission spectra the average width of levels can be effectively used. The strong dependence of the width on many-electron quantum numbers can take place only if some strong Auger transitions are possible for some levels, but forbidden for the other ones, as well as in the case of transitions between the neighbouring shells with the same principle quantum number [10]. The values of average width for the excited $2p^5 3d^{N+1}$ configurations of all $3d$ elements are given in Table 1. For $2p^{-1}$ vacancy the width is determined by Auger transitions; the larger width of the $2p_{1/2}^{-1}$ vacancy is caused by the Coster–Kronig transitions shifting the vacancy to the $2p_{3/2}^{-1}$ subshell. These transitions are forbidden for some levels energetically, thus the averaging has been performed only with respect to the levels from which such transitions are permitted. The contribution of Coster–Kronig transitions is practically negligible for Sc, relatively small for Fe, but it constitutes a half of the average natural width for the levels of $2p_{1/2}^5 3d^9$ configuration for Ni. Due to the small fluorescence yield, the contribution of the radiative transitions is practically negligible, only for Cu it amounts to 0.01 eV.

Sc. The ground configuration has only two levels; at the temperature used the higher $^2\mathrm{D}_{5/2}$ level having larger statistical weight is more populated (56%) than the lower-lying $^2\mathrm{D}_{3/2}$ level (44%). The excited configuration has been considered in five-configuration approximation:

$$2p^5(3d^2 4s^2 + 3d^3 4s + 3d^4 + 3d 4s^2 4d + 3d^2 4p^2)\,. \quad (1)$$

In the expansion for the ground configuration the corresponding admixed configurations except $3d4s^24d$ have been included.

The partial photoexcitation spectra from the both separate ground levels have the similar structure: they consist of three groups of lines or bands formed by overlapping lines (Fig. 1(a, b)). They all are mainly determined by the transitions to the $2p^5 3d^2 4s^2$ configuration, the admixture of other configurations is small. Only several weak lines on the high-energy side of the spectra can be attributed to the transitions to these configurations. The coupling between the $2p_{1/2}^{-1}$ vacancy and the $3d^N$ shell is best described by jj-coupling. In both spectra all lines of the high energy band and almost all lines of the intermediate band correspond to the transitions from the states with the $2p_{1/2}^{-1}$ vacancy, only some weak lines of the intermediate band as well as all structure of the low-energy band correspond to the transitions from the states with the $2p_{3/2}^{-1}$ vacancy. The lines corresponding to the transitions to the same excited levels have almost the same energy and strengthen each other, because the initial ground levels are separated by only 168 cm^{-1}. Thus several most intensive maxima of the total spectrum correspond to such transitions, among them the main maximum at 402.3 eV corresponds to the transitions to the $2p_{3/2}^{-1} 3d^2\ (^1\mathrm{G}_4)\ 2.5$ level. On the other hand, many lines with different energy give a rather complex structure of the summary spectrum.

The total calculated photoexcitation spectrum describes the experimental total ion yield spectrum very

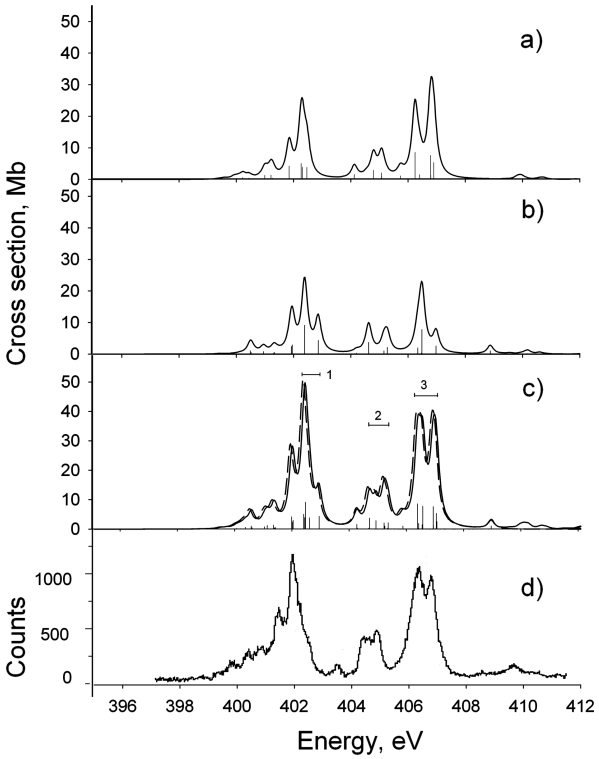

Fig. 1. Sc $2p$ photoabsorption spectrum. Calculation in CI approximation (1): (a) excitation from the $^2D_{3/2}$ level, (b) excitation from $^2D_{5/2}$ level, (c) excitation from the both levels of the ground term (thin line is CI approximation (1), thin broken line is single-configuration approximation, solid line at the higher end of the spectrum is photoionization), (d) experiment [1]. Vertical bars are intensities of lines in CI approximation (1), they have been convoluted using the average natural width. Numbers indicate the intervals of levels used for the excitation of emission spectrum.

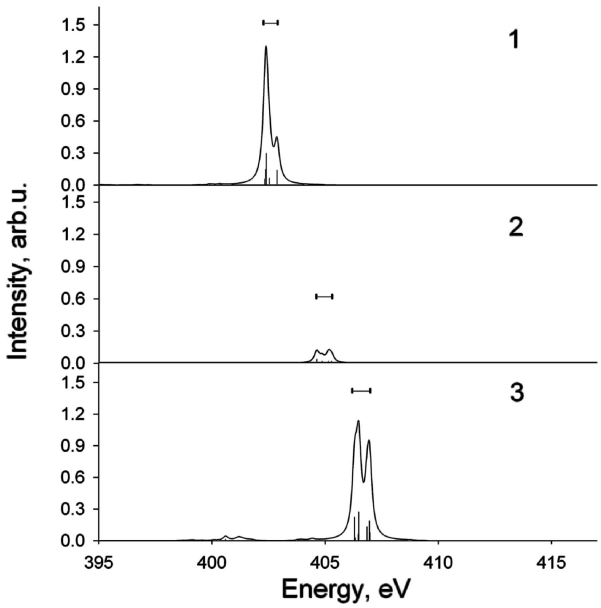

Fig. 2. Sc $L_{2,3}$ emission spectrum generated at the photoexcitation to the groups of levels indicated in Fig. 1: *1* for 402.3–402.9 eV, *2* for 404.6–405.3 eV, *3* for 406.2–407.0 eV. Calculation in CI approximation, lines have been convoluted using the average natural width.

well, only the common shift of 0.5 eV of all calculated spectrum to the higher binding energies takes place [1]. The spectrum is fairly well described even in the single-configuration approximation (Fig. 1(c, d)). Only three small maxima above 409 eV can be attributed to the transitions to admixed configurations. The interpretation of the structure of spectrum using LS-coupling between the $2p^{-1}$ vacancy and the $3d^N$ shell was given in [1].

The photoionization becomes possible only for photon energy from about 411 eV, and its contribution for Sc in the considered interval of energies is negligible. Due to the weakness of photoionization with respect to photoexcitation the emission spectra of Sc and other elements after the ionization have not been considered.

The Coster–Kronig transitions $2p_{1/2}^{-1}$–$2p_{3/2}^{-1}3d^{-1}$ are energetically forbidden, but the $2p_{1/2}^{-1}$–$2p_{3/2}^{-1}4s^{-1}$ transitions are permitted for some levels of the $2p^5 3d^2 4s^2$ configuration. However, due to the small Coster–Kronig width the calculation using individual widths of levels introduces only small differences in the spectrum.

The emission spectra excited by the photon beam at the maxima of absorption spectrum, with the energies corresponding to the intervals indicated in Fig. 1, are plotted in Fig. 2. Under conditions when the ground configuration has only two levels from which the photoexcitation occurs, the emission spectrum in single-configuration approximation contains only the lines at the same energies as the used intervals of the photoexcitation spectrum. In the case *3*, the weak additional structure at the smaller energies appears due to the admixing with other configurations. The transition probability of emission lines is expressed in terms of the same transition amplitudes as the photoexcitation cross-section, but the last one is expressed by the sum of two amplitudes while the first one by single amplitude. Additionally, the intensities of the emission lines also depend on the photoexcitation cross-sections, which define the population of levels. Thus if the excited level is mainly populated by the excitation from one ground level to which the emission takes place, the ratio $I^{\rm em}(i-j)/\sigma^{\rm ex}(i-j)$ obtains a larger value for strong transitions and a smaller value for weak transitions. When the excited levels are populated from the both ground levels this ratio varies insignificantly. The obtained population of the levels of ions after the Coster–Kronig transitions has been by about three or-

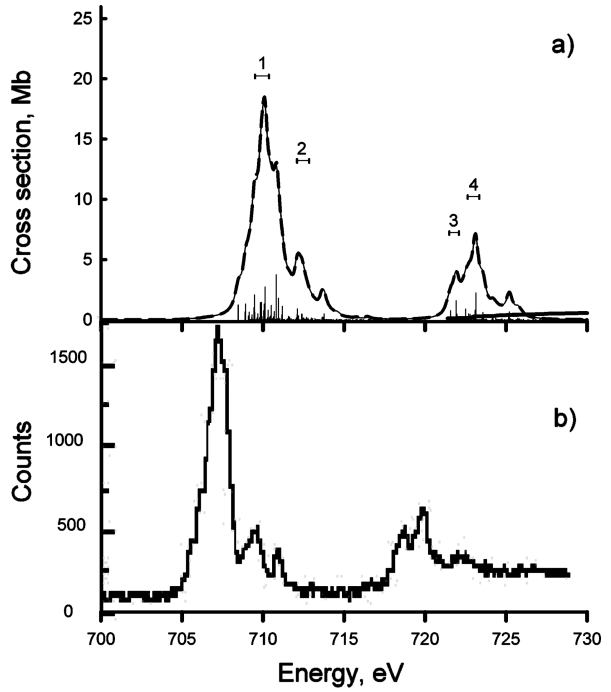

Fig. 3. Fe $2p$ photoabsorption spectrum: (a) calculation (thin line is CI approximation, thin broken line is single-configuration approximation, solid line is photoionization), (b) experiment [2]. Vertical bars are intensities of lines in CI approximation, they have been convoluted using the average natural width. Numbers indicate the intervals of levels used for the excitation of emission spectrum.

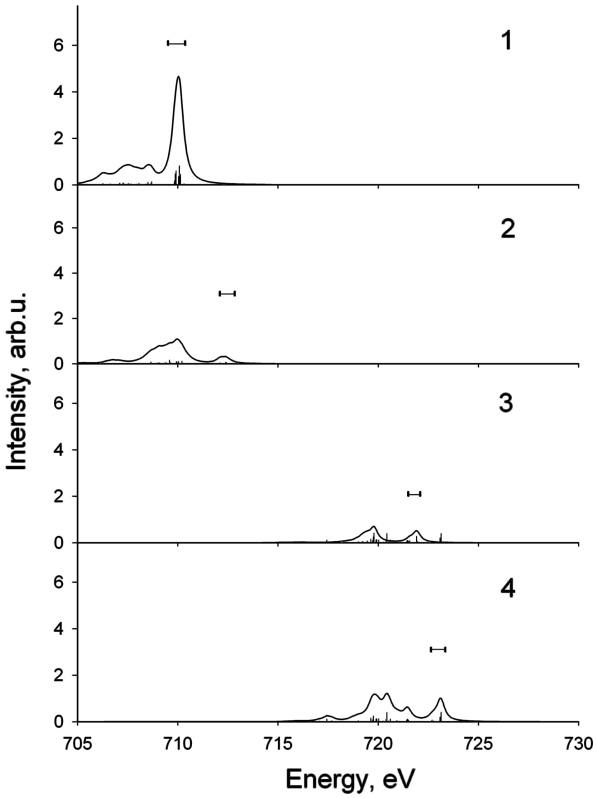

Fig. 4. Fe $L_{2,3}$ emission spectrum generated at the photoexcitation to the groups of levels indicated in Fig. 3: *1* for 709.5–710.4 eV, *2* for 721.5–722.1 eV, *3* for 712.1–712.8 eV, *4* for 722.6–723.4 eV. Calculation in CI approximation, lines have been convoluted using the average natural width.

ders smaller than the population of the levels of atom induced by the photoexcitation. Consequently, the emission of ions practically does not give contribution to the spectrum.

Fe. At the temperature of 1750 K it is necessary to take into account the excitation from all five levels of the ground term; their populations are as follows: ^{5}D$_4$ 48%; ^{5}D$_3$ 27%; ^{5}D$_2$ 15%; ^{5}D$_1$ 8%; ^{5}D$_0$ 2%. For the ground and excited states of transitions the s–d mixing has been taken into account. However, practically all the significant lines can be attributed to the $2p^6 3d^6$–$2p^5 3d^7$ transitions, and the structure of convoluted spectrum changes due to configuration mixing insignificantly (Fig. 3). The contribution of Coster–Kronig transitions increases in comparison to Sc, but all the transitions $2p_{1/2}^{-1}$–$2p_{3/2}^{-1}4s^{-1}$ are permitted energetically and the use of the average width of lines describes fairly well the profile of the photoexcitation as well as the emission spectra.

As a result of the population of many initial levels and the large number of transitions to the final levels of $2p^5 3d^7$ configuration the photoexcitation spectrum consists of many lines. The most intensive lines at 710.16 eV and 726.12 eV correspond to the transitions

$$2p^6 3d^6\,{}^5\mathrm{D}_4 \to 2p^5 3d^7({}^4\mathrm{F}_{4.5})4\,, \quad j = \frac{3}{2}\,, \frac{1}{2}\,. \quad (2)$$

When convoluting the lines with the natural widths, the spectrum obtains the shape of two quasicontinuum bands. Due to the separation of the spin–orbit groups of levels the two bands of spectrum correspond to the transitions from the excited states with $2p_{1/2}^{-1}$ and $2p_{3/2}^{-1}$ vacancies.

The photoionization process becomes possible approximately at the edge of L_3 band, but it is considerably weaker than the photoexcitation and causes only the rise of the high-energy side of this band. Such a rise is characteristic to the experimental spectrum, too.

The emission spectrum has been monitored at four intervals related to the main structure of photoexcitation spectrum (Fig. 4). Besides the transitions inverse to the excitation the additional structure of the spectrum on its low-energy side appears, corresponding to the transitions to the excited levels of ground configuration. Only in the case of excitation at its main maximum the in-

verse transitions to the levels of ground term give the most intensive emission. For the other three intervals the emission is mainly concentrated in the transitions to the excited levels, even to those ones which do not manifest themselves at all in the photoexcitation spectrum.

Ni. Its configuration after the $2p$–$3d$ excitation has only two levels. However, at the temperature of 1800 K the excitation not only from the ground term, but also from the low-lying levels of $3d^9 4s$ configuration must be taken into account. Thus the initial distribution of populations is the following: $3d^8 4s^2\ {}^4\mathrm{F}_4$ 49%, ${}^4\mathrm{F}_3$ 13%, ${}^4\mathrm{F}_2$ 5%, $3d^8 4s\ {}^3\mathrm{D}_3$ 23%, ${}^3\mathrm{D}_2$ 8%, ${}^3\mathrm{D}_1$ 1%.

The excited states have been considered in the following approximation:

$$2p^5(3d^9 4s^2 + 3d^{10} 4s + 3d^9 4p^2)\,. \qquad (3)$$

The same approximation has been applied for the ground states.

The Coster–Kronig transitions, especially the $2p_{1/2}^{-1}$–$2p_{3/2}^{-1} 3d^{-1}$, give the essential contribution to the width of levels, however, they are permitted for all levels, thus the approximation of their widths by the average value

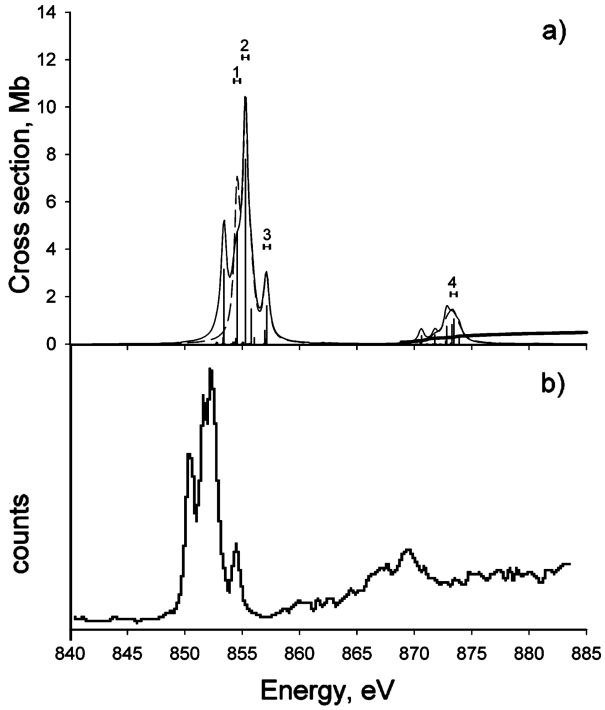

Fig. 5. Ni $2p$ photoabsorption spectrum: (a) calculation (thin line is CI approximation, thin broken line is single-configuration approximation (3), solid line is photoionization), (b) experiment [3]. Vertical bars are intensities of lines in CI approximation, they have been convoluted using the average natural width. Numbers indicate the intervals of levels used for the excitation of emission spectrum.

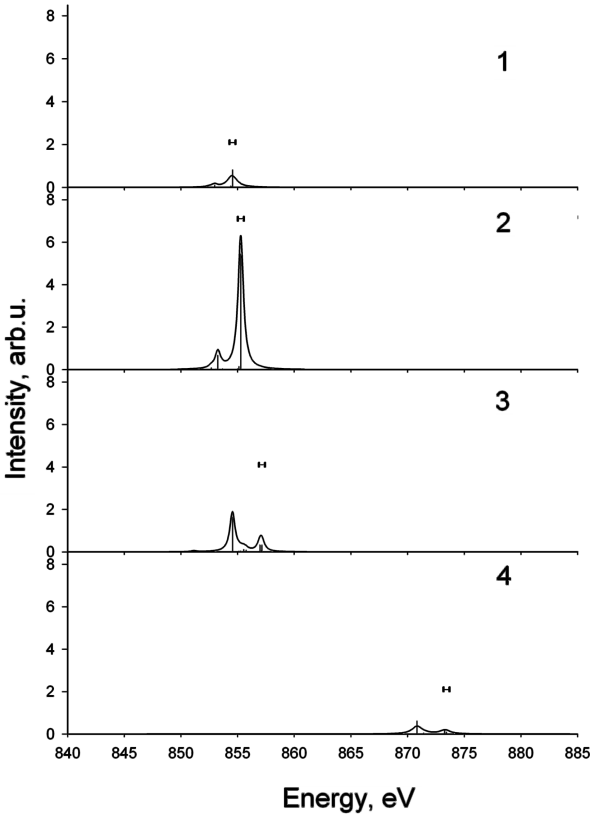

Fig. 6. Ni $L_{2,3}$ emission spectrum generated at the photoexcitation to the levels indicated in Fig. 5: *1* for 854.3–854.8 eV, *2* for 855.0–855.5 eV, *3* for 856.9–857.4 eV, *4* for 873.2–873.7 eV. Calculation in CI approximation, lines have been convoluted using the average natural width.

in calculations of photoexcitation and emission spectra is rather exact.

The photoabsorption spectrum consists of the intensive quasicontinuum band, as well as one distant considerably less intensive band situated at the edge of photoionization continuum (Fig. 5). The interpretation of the structure of spectrum is given in Table 2.

The emission spectrum has been calculated for the excitations using the four intensive lines of absorption spectrum (Fig. 6). In all cases besides the lines of inverse transitions the additional low-energy lines appear; their interpretation is also given in the Table 2. At the excitation with the less intensive lines the additional lines of the emission spectrum become dominating.

3. Conclusions

A promising method to investigate the dynamics of excitation and deexcitation processes in atoms is the monitoring of their emission when exciting near the ionization threshold with the intense monochromatic X-ray beam. The proper object of such investigation

Table 2. Interpretation of the most intensive lines of Ni $2p$ photoabsorption and $L_{2,3}$ emission spectra. Only the lines with intensity exceeding 10% of the most intensive line are included.

Absorption spectrum			
Energy, eV	Cross-section, Mb	Transitions	
		Initial state	Final state
853.41	3.15	$2p^6 3d^9(^2\mathrm{D}_{5/2})4s$ 3.0	$2p^{-1}_{3/2}3d^{10}4s$ 2.0
854.55	4.75	$2p^6 3d^8(^3\mathrm{F}_4)4s^2$ 4.0	$2p^{-1}_{3/2}3d^9_{5/2}4s^2$ 4.0
855.28	7.80	$2p^6 3d^8(^3\mathrm{F}_4)4s^2$ 4.0	$2p^{-1}_{3/2}3d^9_{5/2}4s^2$ 3.0
855.78	1.48	$2p^6 3d^8(^3\mathrm{F}_3)4s^2$ 3.0	$2p^{-1}_{3/2}3d^9_{3/2}4s^2$ 2.0
857.15	1.62	$2p^6 3d^8(^3\mathrm{F}_4)4s^2$ 4.0	$2p^{-1}_{3/2}3d^9_{3/2}4s^2$ 3.0
873.27	0.82	$2p^6 3d^8(^3\mathrm{F}_3)4s^2$ 3.0	$2p^{-1}_{1/2}3d^9_{5/2}4s^2$ 3.0
Emission spectrum			
Energy, eV	Intensity, arb. u.	Transitions	
		Initial state	Final state
853.26	0.68	$2p^{-1}_{3/2}3d^9_{5/2}4s^2$ 3.0	$2p^6 3d^8(^3\mathrm{P}_2)4s^2$ 2.0
853.41	2.24	$2p^{-1}_{3/2}3d^{10}4s$ 2.0	$2p^6 3d^9(^2\mathrm{D}_{5/2})4s$ 3.0
854.55	1.66	$2p^{-1}_{3/2}3d^9_{3/2}4s^2$ 3.0	$2p^6 3d^8(^1\mathrm{G}_4)4s^2$ 4.0
854.55	0.82	$2p^{-1}_{3/2}3d^9_{5/2}4s^2$ 4.0	$2p^6 3d^8(^3\mathrm{F}_4)4s^2$ 4.0
855.28	5.46	$2p^{-1}_{3/2}3d^9_{5/2}4s^2$ 3.0	$2p^6 3d^8(^3\mathrm{F}_4)4s^2$ 4.0
855.785	0.85	$2p^{-1}_{3/2}3d^9_{3/2}4s^2$ 2.0	$2p^6 3d^8(^3\mathrm{F}_3)4s^2$ 3.0
870.83	0.62	$2p^{-1}_{1/2}3d^9_{5/2}4s^2$ 3.0	$2p^6 3d^8(^1\mathrm{G}_4)4p^2$ 4.0

is the $L_{2,3}$ spectra of $3d$ transition elements. Their high resolution $2p$ photoabsorption (photoion yield) spectra of free atoms were recently registered; these are dominated by the $2p$–$3d$ excitation. Contrary to the $3p$ absorption spectra of these elements, the $2p$ photoexcitation spectra are very well described even in the single-configuration approximation. On the other hand, their analysis is complicated due to the population of all levels of the ground term and even of some lowest levels of other configurations in the initial state at the temperatures of evaporation of $3d$ metals. The theoretical investigation of these spectra has been continued in this work, taking into account the photoionization and Auger processes. However, the main aim has been to investigate the emission spectra generated at the energies corresponding to the main maxima of the photoexcitation spectra. The monitoring of the spectra of three different elements Sc, Fe, and Ni from the beginning, middle and end of the $3d$ group has been performed.

In the emission spectrum of Sc all the intense lines are the same as the excitation lines. In the emission spectra of Fe and Ni an additional structure corresponding to the transitions to higher levels of the ground configuration appears. At the excitation corresponding to the less intensive maxima of the photoexcitation spectra the additional structure becomes dominant.

Acknowledgement

This work was partly funded by the European Commission, project RI026715 BalticGrid.

References

[1] B. Obst, T. Richter, M. Martins, and P. Zimmermann, J. Phys. B **34**, L657 (2001).
[2] M. Martins, K. Godehusen, T. Richter, T. Wolff, and P. Zimmermann, J. Electron Spectrosc. Related Phenom. **345**, 137 (2004).
[3] T. Richter, K. Godehusen, M. Martins, T. Wolff, and P. Zimmermann, Phys. Rev. Lett. **93**, 023002 (2004).
[4] M. Martins, K. Godehusen, T. Richter, P. Wernet, and P. Zimmermann, J. Phys. B **39**, R79 (2006).

[5] S. Kučas, A. Kynienė, R. Karazija, L.D. Finkelstein, and E.Z. Kurmaev. J. Phys: Cond. Matter **17**, 7307 (2005).
[6] L.D. Finkelshtein et al., Fiz. Tverd. Tela (St. Petersburg) [Phys. Solid State] **48**, 396 (2006) [in Russian].
[7] K. Godehusen, T. Richter, P. Zimmermann, and M. Martins, Phys. Rev. Lett. **88**, 217601 (2002).
[8] R.D. Cowan, *The Theory of Atomic Structure and Spectra* (C.A. University of California, Berkley, 1981).
[9] S. Kučas, R. Karazija, and A. Kynienė, J. Phys. B **39**, 1711 (2006).
[10] G. Merkelis and R. Karazija, J. Electron Spectrosc. Related Phenom. **67**, 123 (2003).

RENTGENO SPINDULIŲ $L_{2,3}$ EMISIJOS PRIE $2p$ SLENKSČIO MONITORINGAS GELEŽIES GRUPĖS ATOMAMS

A. Kynienė, S. Kučas, R. Karazija

VU Teorinės fizikos ir astronomijos institutas, Vilnius, Lietuva

Santrauka

Intensyvūs Rentgeno spindulių šaltiniai leidžia tirti emisijos spektro kitimą, palaipsniui sužadinant atomus į atskirus energijos lygmenis ar jų grupes, tai yra atlikti vadinamąjį emisijos spektro monitoringą. Šiame darbe nagrinėjama, kaip kinta $L_{2,3}$ spektras, jį sužadinant fotonais prieš $2p$ jonizacijos slenkstį. Tyrimas atliktas trims geležies grupės elementams Sc, Fe ir Ni, kurių atomuose yra skirtingas $3d$ elektronų skaičius, atitinkamai 1, 6 ir 8. Šių elementų laisviesiems atomams gauti reikalinga gana aukšta 1000–1800 K temperatūra, tad reikia priimti dėmesin ne vieno. o kelių žemiausiųjų lygmenų užimtumus. Fotosužadinimo spektro skaičiavimo konfigūracijų sumaišymo artutinumu rezultatai gerai atitinka eksperimentinius spektrus. Tuo remiantis buvo parinktos lygmenų grupės, į kurias sužadinimas yra tikimiausias. Gautuose Sc emisijos spektruose visos linijos, išskyrus kelias silpnas satelitines, atitinka fotosužadinimo spektro linijas. Tuo tarpu daugeliui Fe ir Ni emisijos spektrų yra būdingos intensyvios linijos, atitinkančios šuolius į sužadintus lygmenis.